Magazine of Civil Engineering. 2025. 18(3). Article No. 13508

Magazine of Civil Engineering

journal homepage: http://engstroy.spbstu.ru/

ISSN 2712-8172

Research article

UDC 699.841

DOI: 10.34910/MCE.135.8

Nonlinear seismic response of a reinforced concrete large-panel precast building

Z.K. Abaev [1] , ***B.M. Yazyev*** [2] , ***A.D. Valiev*** [3]

[1] *Vladikavkaz Scientific Centre of the Russian Academy of Sciences, Mikhailovskoye, Prigorodny district, RNO-Alania, Russian Federation*

[2] *Don State Technical University, Rostov-on-Don, Russian Federation*

[3] *North Caucasian Institute of Mining and Metallurgy (State Technological University), Vladikavkaz, RNO-Alania, Russian Federation*

abaich@yandex.ru

Keywords: large-panel buildings, precast reinforced concrete, nonlinear dynamic analysis, seismic performance evaluation

Abstract. This study investigates the seismic performance of reinforced concrete large-panel precast buildings, focusing on their nonlinear response under various earthquake scenarios. The widespread use of Large-Panel Buildings (LPBs) in seismically active regions, coupled with their unique structural properties and limitations of current analysis methods, requires a more comprehensive understanding of their behavior during earthquakes. A detailed numerical model was developed to capture the complex dynamics of LPBs, including nonlinear material properties, panel-to-panel interaction, and connection behavior under dynamic loading. The research methodology used advanced computational techniques, including nonlinear time history analysis and local response examination of critical elements, with a particular focus on connection regions. The results demonstrate significant differences between traditional code-based linear analyses and nonlinear dynamic analyses, especially in predicting damage distribution and interstory drift ratio (IDR). Specifically, the nonlinear analysis revealed a concentration of damage in lower stories, with maximum IDR values of 0.282 % in the first story for high-intensity scenarios, contrasting with the code-based predictions of 0.178 % in the middle stories. Furthermore, the study identified limitations in current industry-standard software, particularly in hysteresis modeling capabilities for LPB-specific behavior. These findings underscore the critical importance of employing nonlinear analysis techniques for accurate seismic performance assessment of LPBs and underscore the need for software enhancements to better represent the unique characteristics of these structures in seismic regions.

Funding: The research was supported by the Russian Science Foundation Project No. 24-79-00087, https://rscf.ru/en/project/24-79-00087

Citation: Abaev, Z.K., Yazyev, B.M., Valiev, A.D. Nonlinear seismic response of a reinforced concrete large-panel precast building. Magazine of Civil Engineering. 2025. 18(3). Article no. 13508. DOI: 10.34910/MCE.135.8

1. Introduction

Large-Panel Buildings (LPBs) have played a key role in the history of urban development and industrial construction worldwide. Introduced in the early 20th century and widely adopted in the post-World War II period, LPBs provided as a rapid and cost-effective solution to acute housing shortages, particularly in Eastern Europe and the former Soviet Union [1]. These structures, characterized by their prefabricated concrete panels assembled on-site, revolutionized the construction industry by offering significantly faster construction and reduced labor costs compared to traditional methods [2].

© Abaev Z.K., Yazyev B.M., Valiev A.D., 2025. Published by Peter the Great St. Petersburg Polytechnic University.

Despite their widespread use and the advantages they offered in terms of construction speed and cost effectiveness, the seismic performance of LPBs has been a subject of ongoing concern and study by structural engineers [3]. Another crucial aspect of LPB seismic behavior is the potential for progressive collapse. Inadequate connection design or its deterioration can lead to disproportionate failure under seismic loads, where the failure of a single structural element may trigger a cascading collapse of a larger portion of the building [4]. This risk underscores the importance of accurate modeling and assessment of connection behavior in LPBs.

Many LPBs have demonstrated surprising resilience during earthquakes, prompting further investigation of their complex behavior under seismic loads [5, 6]. This dichotomy underscores the need for more sophisticated analysis techniques to accurately assess and predict LPB performance in earthquakes. The variability in performance can be attributed to factors such as construction quality, regional design practices, and specific characteristics of seismic events [7].

Analytical studies of LPB seismic performance have evolved significantly over the years, reflecting advancements in both computational capabilities and understanding of structural dynamics. Early research focused on simplified linear models, which, while providing initial insights, failed to capture the full complexity of LPB behavior during seismic events [8]. These models were often based on assumptions that did not adequately represent the unique characteristics of precast panel structures, such as the behavior of connections under dynamic loading.

More recent studies have used advanced numerical methods and nonlinear analysis techniques to better understand the dynamic response of the structures [9]. These analyses have underscored the importance of several critical factors in LPB seismic performance: connection behavior under dynamic loading, panel-to-panel interaction, the influence of openings on overall structural integrity, and nonlinear material properties of precast concrete elements [10]. Taking these factors into account has led to more accurate predictions of LPB behavior under seismic loads but has also revealed the complexity of the problem and the limitations of current analytical tools.

Despite these advancements, there is still a pressing need for more sophisticated and accurate models to predict the seismic response of LPBs. The complexity of these structures, including the interactions between individual panels, the role of connections, and the nonlinear material behavior under extreme loading conditions, requires the development of comprehensive analytical tools [11]. Such models are crucial not only for assessing the safety of existing LPBs but also for developing retrofit strategies and designing new structures in seismic regions [12].

However, current industry-standard software is often unable to accurately model the unique characteristics of LPBs [13]. Common limitations include restricted options for hysteresis models, inability to modify parameters of standard hysteresis models, and a lack of specialized elements for modeling panel connections. These shortcomings can lead to potential misrepresentation of LPB behavior under seismic loads, especially when relying on traditional code-based or linear dynamic analyses [14, 15].

The importance of accurate seismic performance assessment for LPBs cannot be overstated. These structures continue to house millions of people worldwide, often in seismically active regions [16]. The aging of these buildings, combined with evolving seismic design standards, has created an urgent need for reliable assessment methods to inform decisions about renovation, retrofit, or replacement [17].

This study aims to address these challenges by presenting a detailed nonlinear seismic response analysis of a reinforced concrete large-panel precast building. Using state-of-the-art computational methods, the dynamic behavior of a representative LPB under various seismic scenarios is investigated. The analysis includes advanced material models specific to precast concrete behavior, detailed representation of panel connections and sensitivity analysis to damping variations.

By providing a comprehensive understanding of the structure’s response, including potential failure modes and performance limits, this research contributes to the broader goal of enhancing the seismic resilience of LPBs and similar precast concrete structures. The study specifically focuses on developing a numerical model for nonlinear analysis that can represent the particular seismic behavior of LPBs, comparing results from traditional code-based and linear dynamic analyses with those from nonlinear analysis, investigating the sensitivity of structural response to damping variations, analyzing local responses of critical elements (particularly in connection regions), and identifying shortcomings in current analysis software while proposing recommendations for their modernization.

2. Materials and Methods

The object of the study is a typical residential apartment building of reinforced concrete large-panel precast type series 92, located in Vladikavkaz city (Fig. 1): 9-story 1-section building with plan dimensions 24.6×12.6 m. The story height is 3 m. External walls are 300 mm thick panels, internal walls are 160 mm thick single-layer panels, partitions are 80 mm thick. Floor panels are 160 mm thick. Concrete grade – M150 (f_c' = 8.5 MPa, E_c = 24000 MPa), reinforcement – A-I (R_s = 240 MPa, E_s = 200000 MPa).

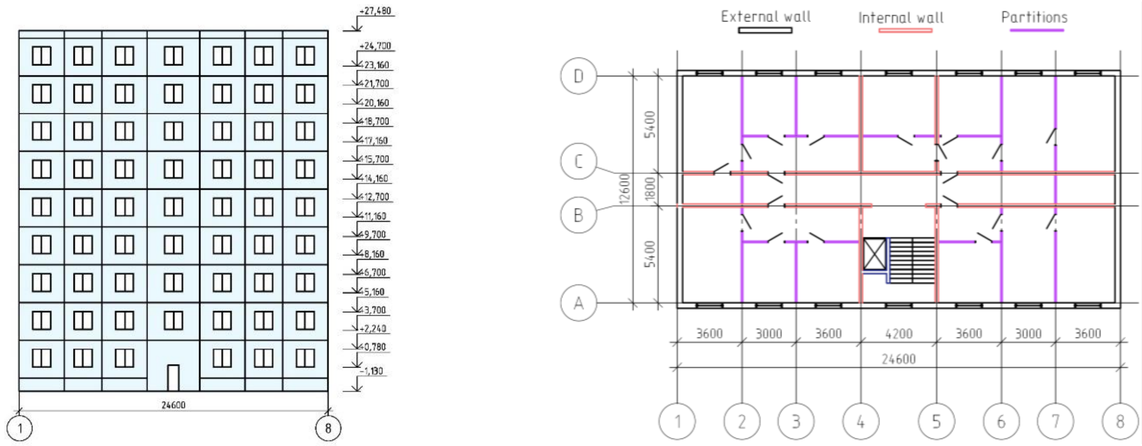

a b

Figure 1. Object of the study: a) elevation, b) plan.

The details of the horizontal and vertical panel connections are shown in Fig. 2.

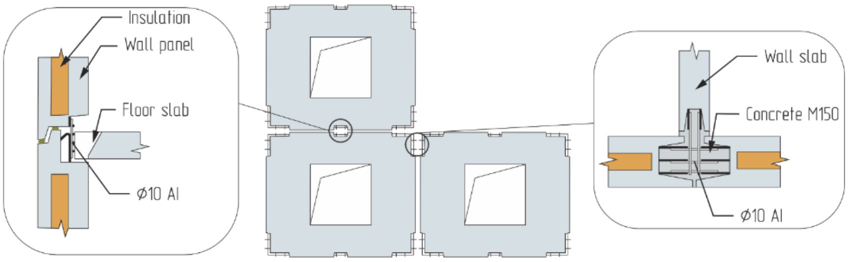

Figure 2. Details of the building.

3. *Modeling Assumptions*

In the modeling of large-panel precast structures, it is conventional to assume that the solid panels exhibit linear elastic behavior. This assumption is justified by the anticipated function of these elements within the structure's overall seismic response. Typically, wall panels are considered to behave in an elastic-brittle manner with respect to in-plane normal forces. Any potential nonlinear or inelastic behavior is often deemed negligible in the panels themselves and is concentrated in the connection regions, where it can be more effectively modeled and analyzed [11].

The floor system acts as a series of rigid diaphragms. The primary objective of the research is to evaluate the building's lateral load-resisting system and the global seismic response of the building. That's why the precast floor panels were replaced by continuous floor that ensures rigid diaphragm action for uniform force distribution, a key factor in global seismic performance [18].

The foundation is rigid.

The following assumptions are made for the connection [19]:

- all points of the horizontal section remain in one plane after the force is applied (plane sections remain plane);
- for the tensile zone of the section, the tensile strength of concrete is not taken into account;
- normal compressive stresses distribution along the section is linear or bilinear.

Linear normal stress distribution is taken when the maximum value of compressive stresses σ_{max} does not exceed the value of compressive strength of concrete R_c. Otherwise, a bilinear diagram consisting of two zones is taken, in the first of which, the compressive stresses change linearly from σ_{min} > 0 (positive values are taken for the compressive stresses) to σ_{max} = R_c, and in the second zone, the values are constant and equal to R_c. During the analysis, it is assumed that within the length of the linear zone, the material of the is elastic, and in the zone where $\sigma_{max} = R_c$, it is in the plastic state.

The bilinear diagram of compressive stress allows to describe all designed situations and includes linear and rectangular diagrams of normal compressive stresses as special cases (Fig. 3).

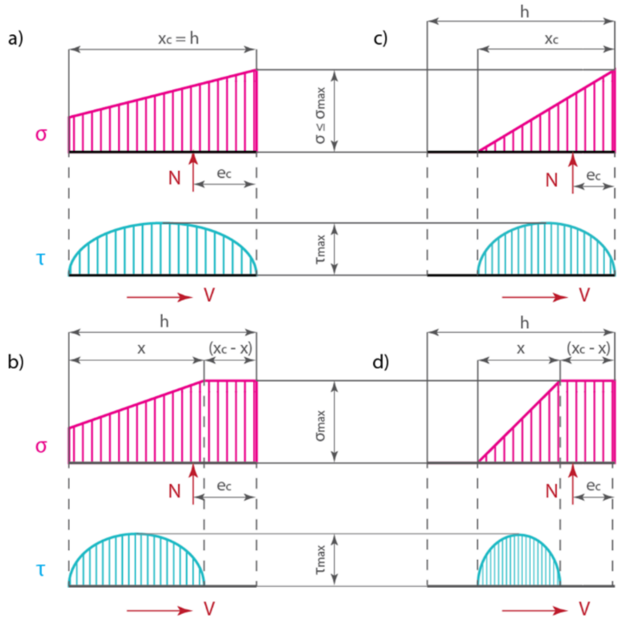

Figure 3. Normal σ and shear τ stress distribution in the horizontal connection in the combined shear-compression action: a), b) compression along the entire length of the section, respectively for linear and bilinear distributions; c), d) compression in portion of the length of the section.

The finite element method software LIRA-SAPR is used for numerical analysis.

Nonlinear behavior of the horizontal connection region is modeled by a combination of two finite elements (FEs) (Fig. 4) [20, 21]:

- 2-node link element (FE 255) for modeling shear keys (Fig. 5);
- shell element (FE 259) representing stress distribution in the connection region (Fig. 6).

The precast walls and floor panels are modeled with elastic shell element (FE 44). The connection behavior between floor and wall panels is modeled without any eccentricity, is also represented using FE 44.

Vertical connections, including shear keys, are simulated using 2-node link elements (FE 255), incorporating the total cross-sectional area of welded reinforcing steel bars to ensure accurate shear transfer [22].

The mechanical properties of FE 255 (for vertical connections) and FE 259 (for horizontal connections) are determined in compliance with the Code of Practice SP 335.1325800.2017 *"Large-panel construction system. Design rules"* (issued by the Ministry of Construction and Housing and Communal Services of the Russian Federation). The parameters presented in Table 1, including stiffness, strength, and deformation capacity, are derived from material properties (concrete grade, reinforcement yield strength) and shear key geometry (dimensions, reinforcement detailing).

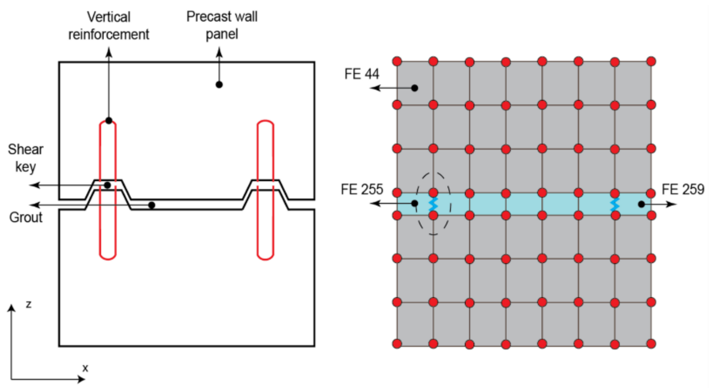

Figure 4. FE implementation of the horizontal connection region in LIRA-SAPR software.

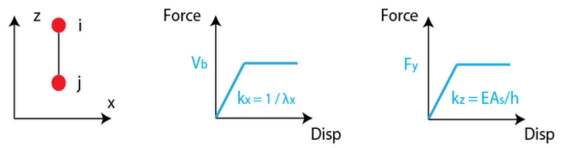

Figure 5. 2-node link element (FE 255).

Table 1. 2-node link element (FE 255) parameters.

Formula	Description
The design shear strength of one shear key: $$V_b = \min \begin{cases} V_{sh,b} = 1.5R_{bt}A_{sh} \\ V_c = R_{b,loc}A_c \\ V_{crc,b} = 0.7R_{bt}A_j \end{cases} \quad (1)$$	$V_{sh,b}$ – shear strength for shear; $V_{c,b}$ – shear strength for crushing; $V_{crc,b}$ – shear strength for shear cracks opening; R_{bt} – design tensile strength of grouting concrete; $R_{b,loc}$ – crushing strength, taken equal $1.5R_b$ – for single keys; A_{sh} – shear area; A_c – crushing area; A_j – cross-sectional area: $A_j = s_{bt}b_{mon}$, where s_{bt} – distance between shear keys; b_{mon} – wall thickness of the grouting area.
The elastic pliability of one shear key: $$\lambda_x^1 = \frac{l_{loc}\left(\frac{1}{E_{b,\omega}} + \frac{1}{E_{b,mon}}\right)}{A_{loc}} \quad (2)$$ The pliability after shear cracks: $$\lambda_x^2 = \frac{6}{d_s n_s}\left(\frac{1}{E_{b,\omega}} + \frac{1}{E_{b,mon}}\right) \quad (3)$$	A_{loc} – loaded area; l_{loc} – shear key height (recommended l_{loc} = 250 mm); E_b – elastic modulus of concrete precast element; $E_{b,mon}$ – elastic modulus of grouting concrete; d_s – connection rebars diameter; n_s – number of the connection rebars.
The elastic stiffness along z-axis: $$k_z = EA_s/h \quad (4)$$	F_y – yield strength of the rebar; E – elastic modulus of the rebar; A_s – rebar cross-sectional area; h – rebar length (equal to the connection height).

$\sigma - \tau$ relation for FE 259 that represents the theoretical assumptions for the connection section described previously are presented in Fig. 6a. In general, FE of platform connection behavior may be described with $\sigma - \varepsilon$ diagram presented in Figs. 6b, 6c.

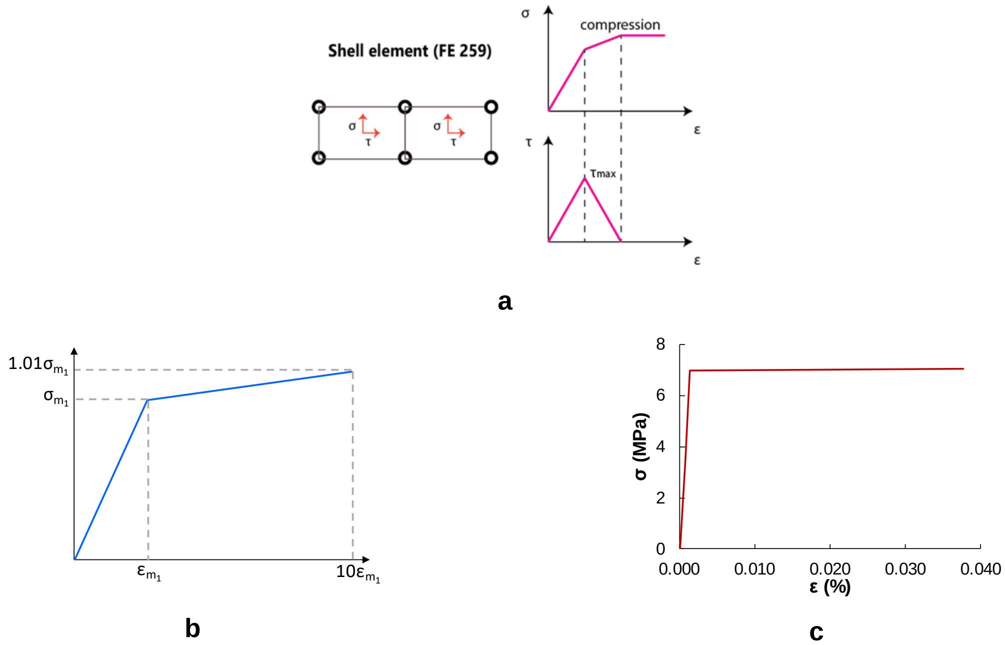

Figure 6. Shell element (FE 259): a) σ-τ relation, b) σ-ε diagram, c) σ-ε diagram for object of study.

During short-term compression for a mortar with a compressive strength of 1 MPa or more, with a connection thickness of 10–20 mm, pliability coefficient of the mortar bed joint λ_m, mm³/N:

$$\text{for } \sigma_m \leq 1.15 R_m^{2/3} - \lambda_m = 1.5 \cdot 10^{-3} R_m^{2/3} t_m; \tag{5}$$

$$\text{for } 2R_m^{2/3} \geq 1.15 R_m^{2/3} - \lambda_m = 5 \cdot 10^{-3} R_m^{2/3} t_m. \tag{6}$$

Pliability coefficient of the connection:

$$\lambda_{c,pl} = \left(\lambda_m + \lambda'_m + \frac{h_{sl}}{E_b} \right) \frac{B_{pl}}{B_{pl} - h_v}, \tag{7}$$

where λ'_m and λ_m – upper and lower mortar bed connection flexibility coefficients; h_{sl} – floor panel height; B_{pl} – contact areas width; h_v – connection width between floor panels.

Strain:

$$\varepsilon = \frac{\lambda_i \sigma_i}{h_v}. \tag{8}$$

Stresses:

$$\sigma_m^1 = 1.15 R_m^{2/3}; \tag{9}$$

$$\sigma_m^2 = 2 R_m^{2/3}; \tag{10}$$

$$\sigma_m^y = 1.01 \sigma_m^2. \tag{11}$$

This study prioritizes overall building performance, where precise opening effects are secondary to the global lateral resistance, therefore, the panels with openings were replaced with solid panels of reduced stiffness. The reduction factor was calculated as the ratio of the wall area with openings to the wall area without the openings. The reduced stiffness accounts for the weakening effect of openings while maintaining computational efficiency. For detailed local stress analysis (e.g., around openings), a refined micro-modeling approach should be adopted, which is the subject of future research. To reduce the computational time, the optimal FE mesh size was determined by considering three mesh sizes: 0.1 m, 0.2 m, and 0.4 m (Table 2). In the case of panels with openings, which complicate the computation by stress concentrations, these panels were replaced with solid panels of reduced stiffness. The reduction factor was calculated as the ratio of the wall area with openings to the wall area without the openings. Mesh sensitivity was conducted for nonlinear dynamic history analysis. The analysis time, maximum displacement and maximum interstory drift ratio (IDR) were compared with the reference model. As a result, the FE mesh of the wall panels was set to 0.4×0.4 m, and the FE mesh of the connections was set to 0.4×0.1 m.

The resulting FE model in LIRA–SAPR is shown in Fig. 7.

The self-weight and live load were applied according to the Code of Practice SP 20.13330.2016 *"Loads and actions"* (issued by the Ministry of Construction and Housing and Communal Services of the Russian Federation).

Table 2. Mesh sensitivity analysis.

No.	Description	Analysis time	Max displacement, mm	Max IDR, %	Error relative to Model 1, %
1	Mesh 0.1×0.1 m with openings	5'40"	93.9	0.457	–
2	Reduced (Mesh 0.1×0.1 m)	5'51"	94.7	0.473	3.383
3	Reduced (Wall Mesh 0.2×0.2 m; Connection Mesh 0.2×0.1 m)	3'10"	94.9	0.476	3.992
4	Reduced (Wall Mesh 0.4×0.4 m; Connection Mesh 0.4×0.1 m)	2'24"	94.8	0.48	4.792
5	Reduced (Wall Mesh 0.1×0.1 m; Connection Mesh 0.2×0.1 m)	5'32"	94.3	0.48	4.796
6	Reduced (Wall Mesh 0.1×0.1 m; Connection Mesh 0.4×0.1 m)	5'10"	91.9	0.48	4.79
7	Reduced (Wall Mesh 0.2×0.2 m; Connection Mesh 0.4×0.1 m)	3'19"	94.1	0.483	5.383

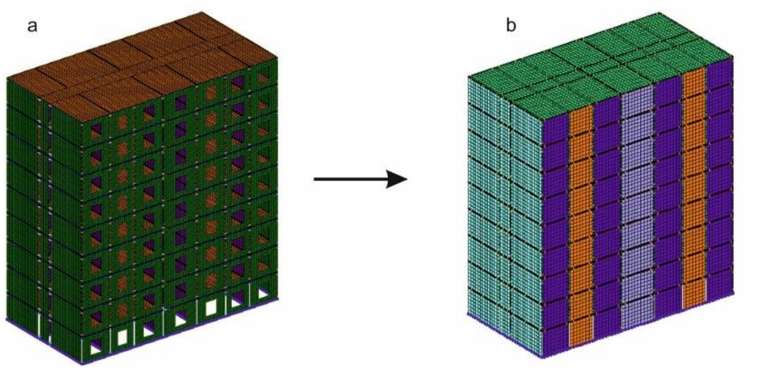

Figure 7. FE model of the building in LIRA-SAPR software: a) initial model with openings, b) model with solid panels.

4. Analysis Methods

The model was subjected to two components of ground motion of the 1988 Spitak, Armenia, earthquake (Figs. 7, 8). The earthquake, with a surface wave magnitude of 6.8 and a maximum MSK-64 intensity of *X* (Devastating), occurred in the northern part of the Armenian Republic of the Soviet Union on December 7, 1988, resulting in thousands of deaths and injuries [23]. The ground acceleration records are shown in Figs. 8, 9.

The following load cases were applied to the building model:

- Nonlinear dynamic analysis for two components of unscaled ground motion.
- Linear dynamic analysis for two components of unscaled ground motion.
- Linear code-based analyses according to the Code of Practice SP 14.13330.2018 *"Seismic building design code"* (issued by the Ministry of Construction and Housing and Communal Services of the Russian Federation) for intensity levels VII, VIII, IX of the MSK-64 scale.
- Linear response spectrum analysis for unscaled ground motion response spectrum shown in Fig. 10.

Four different damping ratio values were investigated in nonlinear dynamic load case, namely 2, 3, 4, 5 % of critical damping.

The ground motion was scaled for three different intensity levels for nonlinear dynamic load case with 5 % of critical damping to compare with code-based analyses, namely 0.1 g, 0.2 g, and 0.4 g.

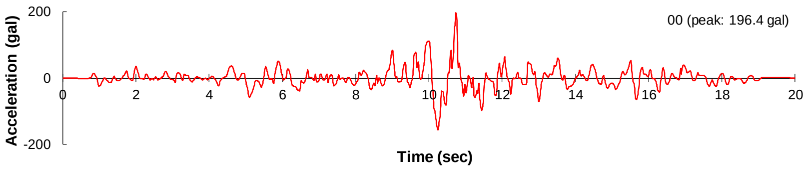

Figure 8. Ground acceleration record (Spitak, Armenia, 1988, Gukasian station, component 000).

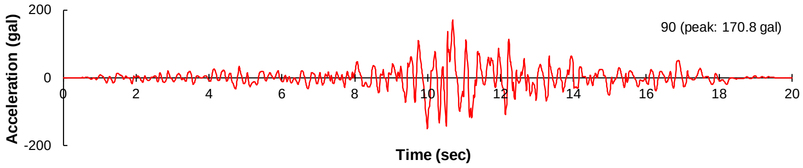

Figure 9. Ground acceleration record (Spitak, Armenia, 1988, Gukasian station, component 090).

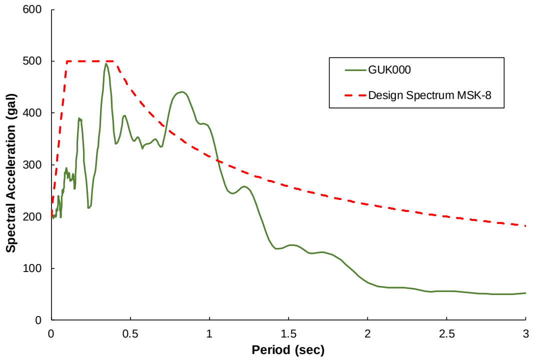

Figure 10. Response spectrum (Spitak, Armenia, 1988, Gukasian station, component 000).

The nonlinear and linear analyses were performed using an explicit integration of the equation of motion [24]:

$$M\ddot{x}+C\dot{x}+Kx=-Mea_0\left(t\right), \quad (12)$$

where $x=u$ – unknown vector of nodal displacements; $\dot{x}=v$ – nodal velocity vector; $\ddot{x}=a$ – nodal acceleration vector; $a_0\left(t\right)$ – ground acceleration; e – direction cosines vector; M – mass matrix; C – damping matrix; K – stiffness matrix.

Analysis parameters:

- Newmark-beta method (average constant acceleration with γ = 0.5 and β = 0.25) is used for direct integration of the equations of motion.
- Modified Newton–Raphson method is used for solving nonlinear equations at each time step.

LIRA-SAPR offers two predefined hysteresis models for nonlinear analyses: a peak-oriented model and an isotropic hardening model (Figs. 11a and 11b, respectively). For the current study, the peak-oriented hysteretic model (Fig. 11a) is used [25].

However, it is crucial to underscore a significant limitation of LIRA-SAPR: the inability to modify or customize the analytical parameters and parameter of these standard hysteresis models. While this constraint may be acceptable for conventional structures, it presents a considerable challenge when analyzing LPBs and other precast panel structures. LPBs exhibit unique strength and stiffness degradation behaviors that deviate from those of monolithic structures, primarily due to their distinct assembly methods and connection characteristics [26].

- Total integration time is 20 sec.
- Integration step is 0.01 sec.

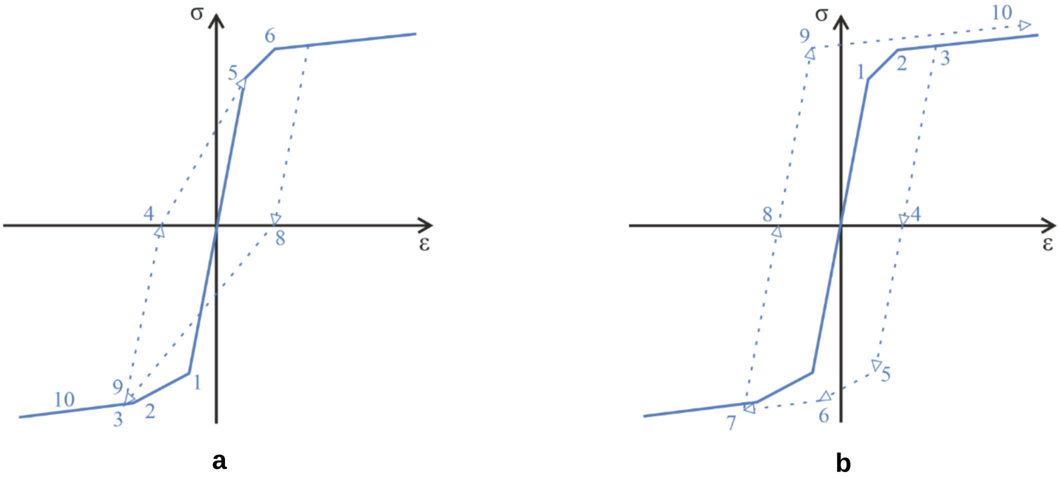

Figure 11. LIRA-SAPR's hysteresis models: a) peak-oriented model, b) isotropic hardening model.

5. Results and Discussion

The natural period of the structure is 0.367 sec in the Y direction (short), the second mode period is 0.211 sec in the X direction (long). The mode shapes are shown in Fig. 12.

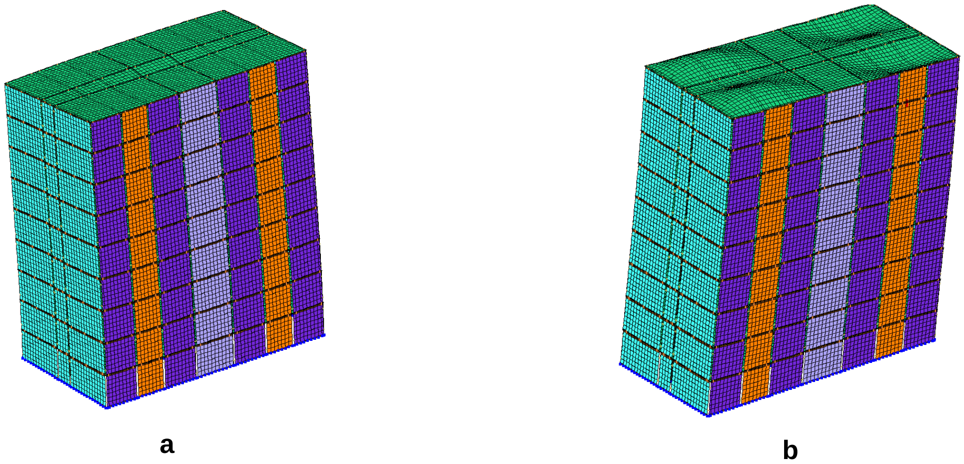

Figure 12. Mode shapes: a) first mode shape (T_1 = 0.37 sec), b) second mode shape (T_2 = 0.21 sec).

Fig. 13 illustrates the maximum displacement profiles for various analytical approaches: nonlinear and linear dynamic analyses, code-based MSK-8, and response spectrum methods. The results demonstrate good correlation along the building height, with slightly elevated values for the nonlinear case.

Notably, the roof displacement time history (Fig. 14) reveals significant discrepancies between linear and nonlinear dynamic load cases. While maximum positive displacements are comparable (19.5 mm for linear, 20.2 mm for nonlinear), the negative displacement in the nonlinear case is approximately half that of the linear case (–9.5 mm vs –18.9 mm, respectively).

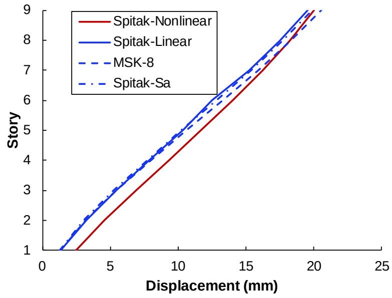

Figure 13. Displacements for different load cases.

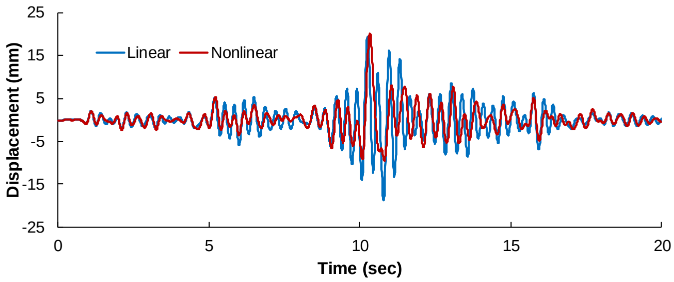

Figure 14. Roof displacement.

A critical finding pertains to the IDR response under varying seismic intensities. The IDR, a key indicator of structural damage [27], exhibits marked differences in both distribution and magnitude across analytical methods. Code-based analyses predict maximum IDR at mid-height, whereas nonlinear analyses indicate peak IDR in the first story. This disparity intensifies with increasing seismic intensity. For instance, under MSK-8 loading, the maximum IDR is 0.089 % (6th story) in code-based analysis versus 0.085 % (1st story) in the 0.2 g nonlinear case. For MSK-9, these values diverge further: 0.178 % (6th story) in code-based analysis compared to 0.282 % (1st story) in the 0.4 g nonlinear case. The damage pattern predicted by the nonlinear analysis, with concentration in the lower stories, aligns closely with observations from post-earthquake inspections of large panel buildings [28], lending further credence to the nonlinear approach.

These findings underscore the critical importance of nonlinear analyses in seismic performance evaluation, as traditional code-based analyses may yield potentially misleading results, particularly in damage distribution prediction and IDR estimation.

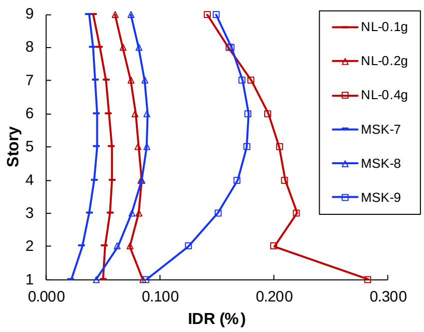

Figure 15. IDR for different load cases.

The graph of the IDR (Fig. 16) exhibits a similar pattern across different damping values, with the maximum drift occurring at the first story. However, the differences in these values are significant, with variations up to 25 %. This notable discrepancy underscores the importance of accurately determining the appropriate damping ratio, which necessitates thorough investigation in future research.

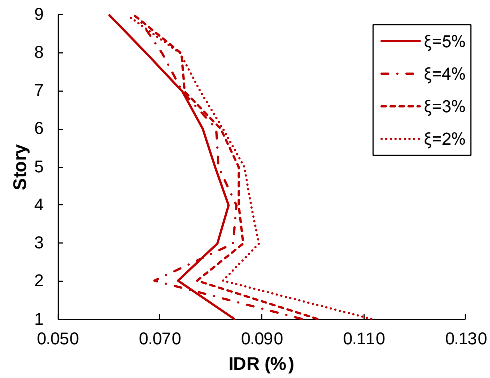

Figure 16. IDR for different damping ratios.

Despite the disparity in IDR values, the overall response in both cases remains relatively low when compared to the commonly accepted ranges for performance-based design as specified by building codes [29]. However, it is important to note that there are currently no established acceptance criteria specifically tailored for LPBs, underscoring the urgent need for the development of such criteria. These should account for the unique behavior and fragility characteristics of this structural type.

The local response of the connection region in the corner panel of the first story was examined for nonlinear dynamic load case. Particular attention was given to the behavior of specific FE within this critical area.

Fig. 17 illustrates the axial stress response for **FE 259**. The observed stress state is exclusively compressive, aligning with the initial modeling assumptions and the desired connection behavior. The ultimate strength of the element is 7100 kPa, while the maximum response reached 3071 kPa. This response indicates that the element experienced low to medium damage, which is consistent with the observed damages [7].

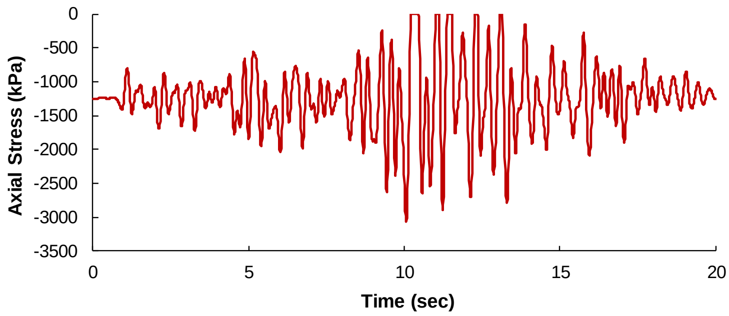

Figure 17. Axial stress response for FE 259.

The shear force response of the shear key element (FE 255) is depicted in Fig. 18. The ultimate shear strength of this element, as calculated using equation (1), is 45 kN. Fig. 19 presents the relationship between shear force and shear deformation for this element. The data indicate that the element attained its ultimate strength, suggesting the possibility of shear key failure [30]. It is noteworthy that the peak response for **FE 259** was recorded at approximately the same time step, underscoring the interaction between axial and shear responses in the connection region.

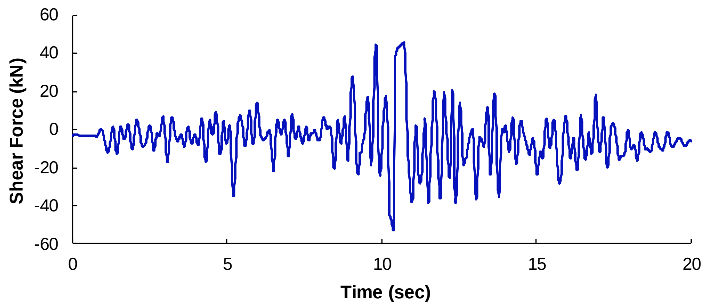

Figure 18. Shear force response for FE 255.

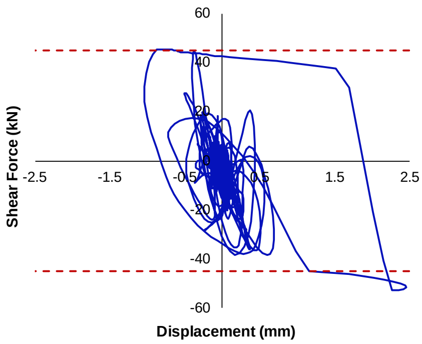

Figure 19. Hysteresis for FE 255.

6. Conclusions

The findings of this paper contribute to the understanding of LPBs seismic behavior and underscore the critical importance of nonlinear analysis in accurately assessing and predicting the seismic performance of these structures.

1. A comprehensive numerical model for nonlinear seismic analysis of LPBs was successfully developed. This model effectively captured the unique seismic behavior of LPBs, including panel-to-panel interactions, nonlinear material properties, connection behavior under dynamic loading.
2. Substantial differences were observed between traditional code-based and linear dynamic analyses versus nonlinear analysis:
   - IDR distribution: code-based analyses predicted maximum IDR at mid-height, while nonlinear analyses indicated peak IDR in the first story.
   - IDR magnitude: for MSK-9 intensity, code-based analysis predicted a maximum IDR of 0.178 % (6^{th} story), whereas nonlinear analysis for 0.4 g PGA showed 0.282 % (1^{st} story).
   - Damage pattern: nonlinear analysis results aligned closely with post-earthquake observations, predicting concentration of damage in lower stories.
3. These results underscore the importance of nonlinear analysis in accurately predicting LPB behavior under varying seismic intensities.
4. The notable discrepancy in response for different damping ratios (up to 25 %) was observed for the model.
5. Examination of local responses in critical elements provided valuable insights:
   - Shell element FE 259 (axial stress): maximum response of 3071 kPa, indicating low to medium damage state.
   - 2-node link element FE 255 (shear force): reached ultimate shear strength of 45 kN, suggesting potential shear key failure.
   - Correlation observed between peak responses of FE 259 and FE 255, indicating interaction between axial and shear responses in connection regions.
6. To improve the accuracy of LPB seismic analysis, the following software modernizations are recommended:
   - Implementation of flexible, user-customizable hysteresis models.
   - Development of specialized elements for modeling panel connections and connections.
   - Enhancement of post-processing capabilities for detailed local response analysis.

References

1. Malaia, K. A Unit of Homemaking: The Prefabricated Panel and Domestic Architecture in the Late Soviet Union. Architectural Histories. 2020. 8(1). Article no. 12. DOI: 10.5334/ah.453
2. Malazdrewicz, S., Ostrowski, K.A., Sadowski, Ł. Large Panel System Technology in the Second Half of the Twentieth Century – Literature Review, Recycling Possibilities and Research Gaps. Buildings. 2022. 12(11). Article no. 1822. DOI: 10.3390/buildings12111822
3. Pekau, O.A. Structural integrity of precast panel shear walls. Canadian Journal of Civil Engineering. 1982. 9(1). Pp. 13–24. DOI: 10.1139/l82-002
4. Shapiro, G.I., Gasanov, A.A. Numerical solution of the problem of stability of the prefabricated building against progressive collapse. International Journal for Computational Civil and Structural Engineering. 2016. 12(2). Pp. 158–166.

5. Velkov, M. Behaviour of large panel building during the Romania earthquake of March 4, 1977. IABSE Symposium: Seminar on constructions in seismic zones. 1978. Pp. 32–42. DOI: 10.5169/SEALS-24183
6. Guri, M., Brzev, S., Lluka, D. Performance of Prefabricated Large Panel Reinforced Concrete Buildings in the November 2019 Albania Earthquake. Journal of Earthquake Engineering. 2022. 26(11). Pp. 5799–5825. DOI: 10.1080/13632469.2021.1887010
7. Freddi, F., Novelli, V., Gentile, R., Veliu, E., Andreev, S., Andonov, A., Greco, F., Zhuleku, E. Observations from the 26th November 2019 Albania earthquake: The earthquake engineering field investigation team (EEFIT) mission. Bulletin of Earthquake Engineering. 2021. 19(5). Pp. 2013–2044. DOI: 10.1007/s10518-021-01062-8
8. Clough, R.W., Malhas, F., Oliva, M.G. Seismic Behavior of Large Panel Precast Concrete Walls: Analysis and Experiment. PCI Journal. 1989. 34(5). Pp. 42–66. DOI: 10.15554/pcij.09011989.42.66
9. Cao, P., Kozinetc, G.L., Badenko, V.L., Markov, A., Zotov, D.K., Kozinets, P.V. Dynamic characteristics of a reinforced concrete frame under vibration load conditions. Magazine of Civil Engineering. 2024. 17(2). Article no. 12607. DOI: 10.34910/MCE.126.7
10. Baranski, J., Szolomicki, J., Latka, P. Numerical Analysis of the Joints of Prefabricated Elements in Large-Panel Buildings Located on the Areas of Mining Damages. Proceedings of the World Congress on Engineering and Computer Science. 2. San Francisco, 2017. Pp. 847-852.
11. Becker, J.M., Llorente, C., Mueller, P. Seismic response of precast concrete walls. Earthquake Engineering & Structural Dynamics. 1980. 8(6). Pp. 545–564. DOI: 10.1002/eqe.4290080605
12. Abaev, Z.K., Kodzaev, M.Y., Bigulaev, A.A. Earthquake resistance analysis of structural systems of multi-storey civil buildings. Structural Mechanics of Engineering Constructions and Buildings. 2020. 16(1). Pp. 76–82. DOI: 10.22363/1815-5235-2020-16-1-76-82
13. Abaev, Z., Valiev, A., Kodzaev, M. Methodology of the reinforced concrete large panel buildings modeling with SAPFIR-generator visual programming tool. AIP Conference Proceedings. 2023. 2833(1). Article no. 020024. DOI: 10.1063/5.0151656
14. Powell, G.H. Modeling for Structural Analysis: Behavior and Basics. Computers and Structures Inc. Berkeley, 2010. 365 p.
15. Yu, S., Zhang, Y., Bie, J., Zhang, W., Jiang, J., Chen, H., Chen, X. Finite Element Analysis of Hysteretic Behavior of Superposed Shear Walls Based on OpenSEES. Buildings. 2023. 13(6). Article no. 1382. DOI: 10.3390/buildings13061382
16. Srikanth, K., Borghate, S.B. Review on seismic performance evaluation of precast concrete buildings. Materials Today: Proceedings. 2023. DOI: 10.1016/j.matpr.2023.04.106
17. Wardach, M., Krentowski, J.R., Knyziak, P. Degradation Analyses of Systemic Large-Panel Buildings Using Comparative Testing during Demolition. Materials. 2022. 15(11). Article no. 3770. DOI: 10.3390/ma15113770
18. Rybakov, V., Lalin, V., Pecherskikh, M., Saburov, D. Accounting for rotational inertia in calculating structures for seismic impact. AIP Conference Proceedings. 2023. 2612(1). Article no. 040034. DOI: 10.1063/5.0113989
19. Ashkinadze, G.N., Sokolov, M.E., Martynova, L.D. Zhelezobetonnye steny seismostoikikh zdanii [Reinforced concrete walls of earthquake-resistant buildings]. Moscow: Stroyizdat, 1988. 504 p.
20. Gubchenko, V.E. Work with the 'joint' tool of software package LIRA-CAD. Zhilishchnoe Stroitel'stvo [Housing Construction]. 2018. 3. Pp. 30–35. DOI: 10.31659/0044-4472-2018-3-30-35
21. Vodopianov, R.Yu. Simulation and computation of large-panel buildings in PC LIRA-SAPR 2017. Zhilishchnoe Stroitel'stvo [Housing Construction]. 2017. 3. Pp. 42–48.
22. Rybakov, V.A., Tsvetkova, A.A. Stiffness of vertical keyed joints of large panel buildings before cracking. Construction of Unique Buildings and Structures. 2024. 3(112). Article no. 11201. DOI: 10.4123/CUBS.112.1
23. Noji, E.K. The 1988 Earthquake in Soviet Armenia: Implications for Earthquake Preparedness. Disasters. 1989. 13(3). Pp. 255–262. DOI: 10.1111/j.1467-7717.1989.tb00715.x
24. Chopra, A.K. Dynamics of Structures: Theory and Applications to Earthquake Engineering. 5th ed. Pearson. Hoboken, 2016. 960 p.
25. Lee, C.S., Han, S.W. An Accurate Numerical Model Simulating Hysteretic Behavior of Reinforced Concrete Columns Irrespective of Types of Loading Protocols. International Journal of Concrete Structures and Materials. 2021. 15. Article no. 5. DOI: 10.1186/s40069-020-00446-5
26. Abaev, Z., Valiev, A., Kodzaev, M. Large Panel Reinforced Concrete Buildings Inelastic Behavior Modeling Approach for Nonlinear Seismic Analysis. Lecture Notes in Civil Engineering. 2024. 400. Proceedings of the 7th International Conference on Construction, Architecture and Technosphere Safety. Pp. 162–174. DOI: 10.1007/978-3-031-47810-9_16
27. Yu, X., Li, X., Bai, Y. Evaluating maximum inter-story drift ratios of building structures using time-varying models and Bayesian filters. Soil Dynamics and Earthquake Engineering. 2022. 162. Article no. 107496. DOI: 10.1016/j.soildyn.2022.107496
28. Fintel, M. Performance of Buildings With Shear Walls in Earthquakes of the Last Thirty Years. PCI Journal. 1995. 40(3). Pp. 62–80. DOI: 10.15554/pcij.05011995.62.80
29. Magliulo, G., D'Angela, D., Lopez, P., Manfredi, G. Nonstructural Seismic Loss Analysis of Traditional and Innovative Partition Systems Housed in Code-conforming RC Frame Buildings. Journal of Earthquake Engineering. 2021. 26(15). Pp. 7715–7742. DOI: 10.1080/13632469.2021.1983488
30. Soudki, K.A., Rizkalla, S.H., LeBlanc, B. Horizontal Connections for Precast Concrete Shear Walls Subjected to Cyclic Deformations Part 1: Mild Steel Connections. PCI Journal. 1995. 40(4). Pp. 78–96. DOI: 10.15554/pcij.07011995.78.96

Information about the authors:

Zaurbek Abaev*, PhD in Technical Sciences*
ORCID: https://orcid.org/0000-0002-6932-2740
E-mail: abaich@yandex.ru

Batyr Yazyev*, Doctor of Technical Sciences*
ORCID: https://orcid.org/0000-0002-5205-1446
E-mail: ps62@yandex.ru

Azamat Valiev,
ORCID: https://orcid.org/0000-0002-9436-3691
E-mail: azamatva1@yandex.ru

Received: 24.10.2024. Approved: 15.05.2025. Accepted: 15.05.2025.